Improved Reconstruction of Deep Space Images via Genetic Algorithms

Shawn Aldridge, Brendan Babb, Frank Moore
Mathematical Sciences Dept.
University of Alaska Anchorage
Anchorage, AK, USA
affwm@uaa.alaska.edu

Michael R. Peterson
Computer Science Dept.
University of Hawai'i at Hilo
Hilo, HI, USA
mrp@hawaii.edu

***Abstract*—Most of the images transmitted from deep space probes to Earth are subject to lossy compression. Recent NASA missions (such as Mars rovers *Spirit* and *Opportunity*) have used the ICER progressive wavelet image compressor to achieve state-of-the-art compression performance. The purpose of the research described in this paper was to demonstrate that it is possible to evolve wavelet and scaling numbers describing novel transforms that outperform the most commonly used ICER wavelet for the reconstruction of deep space images previously subjected to lossy compression. Because our technique only modifies the image reconstruction transform, it requires no modification of deployed mission hardware. We thus present a technique to provide improved reconstruction of images received from existing rover missions.**

Keywords-image compression; wavelets; genetic algorithms

I. INTRODUCTION

The National Aeronautics and Space Administration (NASA) Mars Exploration Rovers (MERs) *Spirit* and *Opportunity* (Fig. 1) have been a tremendous success. Since landing on opposite sides of the planet in January 2004, these rovers have been transmitting visual and infrared images of the Martian landscape to Earth. Scientists at NASA's Jet Propulsion Laboratory (JPL) have used these images to discover conclusive evidence of past water activity, suggesting that conditions on Mars may have once been suitable for sustaining life. Each rover is configured with nine onboard cameras. The enormous amount of image data captured by these cameras (as of May 25, 2010, over 128,000 images) and the vast distance over which that data must be transmitted (approximately 100-380 million km) make compression essential. MER scientists often prefer lossy compression schemes because they are capable of achieving significantly greater compression ratios than lossless schemes; unfortunately, this additional compression comes at the cost of introducing distortion into reconstructed images.

ICER [8] is a state-of-the-art wavelet-based progressive image compressor developed by Drs. Aaron Kiely and Matthew Klimesh at JPL specifically for deep-space imaging. Both MERs are relying upon ICER exclusively to perform lossy image compression in order to maximize return of scientific imagery over severely constrained deep space communication links. In addition, ICER is being used by the Sun Earth Connection Coronal and Heliospheric Investigation (SECCHI) instrument onboard NASA's Solar Terrestrial Relations Observatory (STEREO) spacecraft [12] to observe the solar corona and inner heliosphere from the surface of the Sun to the orbit of Earth, and by the Hyperion hyperspectral imager onboard the Earth Observing-1 (EO-1) spacecraft [13] to evaluate on-orbit issues for imaging spectroscopy and assess the capabilities of a space-based imaging spectrometer for earth science and earth observation missions.

At the core of ICER is a collection of seven wavelet transforms. While an ICER user has the option of selecting any these wavelets and specifying a desired multiresolution analysis (MRA) decomposition level, in practice only one of these wavelets has seen extensive use during the current MER missions. The scaling (*h2*) and wavelet (*g2*) numbers defining the low-pass and high-pass synthesis filters for the reconstruction transform of this wavelet – commonly called the reversible 2/6 (TS) due to its simple biorthogonal structure – can be expressed in one of two forms:

(a) The floating-point representation [14] consists of the following values (rounded to eight decimal places):
h2 = [0.70710700, -0.70710700, 0.08838800, 0.08838800, 0.70710678, 0.70710678]

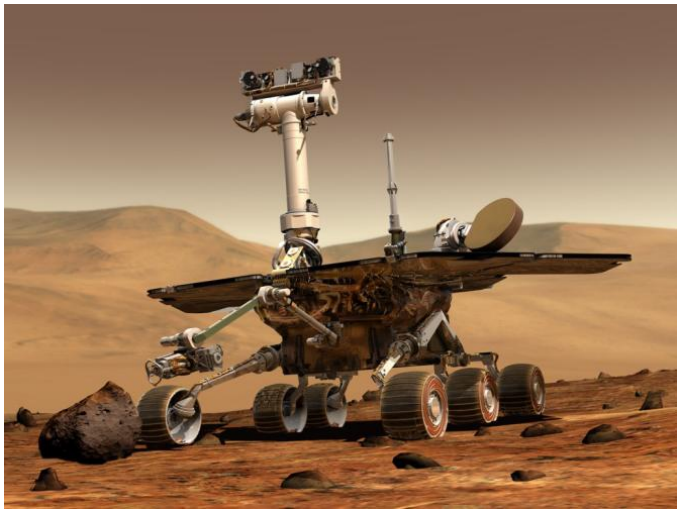

Figure 1. Artist's Concept of a Rover on Mars

g2 = [-0.08838800, -0.08838800]

(b) An alternative integer representation [1], used onboard MERs to reduce computational complexity [8], consists of the following values:
h2 = [1, -1, 1/8, 1/8, 1/2, 1/2]
g2 = [-1/8, -1/8]

Quantization [9] is the process of approximating a signal using a relatively smaller number of bits. Digital audio signals, for example, are commonly represented using either 8 bits (allowing one of 2^8 = 256 possible volume levels) or 16 bits (allowing 2^{16} = 65,536 levels). Fewer bits are used when high fidelity may be sacrificed to improve transmission speed and reduce storage size. Quantization introduces permanent, irreversible information loss. The goal of this research project is to utilize genetic algorithms (GAs) to evolve wavelet and scaling numbers defining novel image reconstruction transforms that outperform the 2/6 wavelet for the reconstruction of deep space images that have previously compressed by the 2/6 and then subjected to quantization error. Performance of the evolved transforms will be measured by distortion, quantified in this research by mean squared error (MSE) introduced into the reconstructed images.

II. Prior Research

A series of research projects begun in 2004 has focused upon using EC to evolve sets of wavelet and scaling numbers describing new transforms capable of reducing the mean squared error (MSE) observed in reconstructed signals subjected to quantization error, while continuing to match or exceed the compression capabilities of wavelets. Moore [10] used a genetic algorithm (GA) to optimize reconstruction transforms only, and demonstrated modest improvements over wavelet reconstruction transforms at various quantization levels. Babb, Becke, and Moore [2] expanded this GA to simultaneously evolve matched compression and reconstruction transform pairs, and added the capability of evolving MRA transforms [11]. Their approach seeded the initial population with one exact copy and many randomly mutated copies of a selected wavelet; thus, each of the transforms in the evolving population had the same structure as the wavelet, but contained different wavelet and scaling numbers. For MRA transforms [9], it proved to be advantageous to evolve different coefficients at every multiresolution level. Evolving a four-level matched compression and reconstruction transform having the same structure as the famous 9/7 transform [5], for example, requires simultaneous optimization of 128 floating-point numbers, which is an extraordinarily difficult problem.

In their best result to date [3], Babb *et al.* used selected satellite images for training under conditions subject to 64:1 quantization. Their best-of-run evolved transform reduced MSE in reconstructed satellite images by an average of 33.78% (1.79 dB) in comparison to the 9/7 wavelet at a single level of decomposition, while maintaining the average information entropy (IE) – a reliable indicator of compressed file size – at 99.57% compared to the 9/7. This transform was also evaluated on 80 fingerprints from the FBI fingerprint image test suite, as well as 18 digital photographs. At 64:1 quantization, the evolved transform reduced the average MSE in reconstructed fingerprints by 49.88% (3.00 dB) in comparison to the 9/7, but allowed the average IE of compressed fingerprints to increase to 104.36%. For the photographs, the evolved transform reduced average MSE by 42.35% (2.39 dB) and maintained average IE at 100.08% in comparison to the 9/7. These results indicate that their evolved transform greatly improved the quality of reconstructed images without substantial loss of compression capability over a broad range of image classes. In addition, their best evolved 3-level MRA transform reduced MSE by an average of 11.71% (0.54 dB) when applied to 50 satellite images from their test set, while maintaining an average IE of 99.47% in comparison to the 9/7 wavelet under conditions subject to 64:1 quantization [4]. Thus, their approach was successfully extended to evolve MRA transforms that reduce MSE in reconstructed images, while continuing to match the compression capabilities of the 9/7.

III. Experiments and Results: 2/6

For this research, the test set consisted of 50 images taken by five cameras aboard MER *Spirit*: the navigation camera (images 1-10), rear hazard camera (11-20), front hazard camera (21-30), panoramic camera (31-40), and microscopic imager camera (41-50). These images were transmitted to Earth under lossless conditions. 50 independent training runs of our GA were performed. Each GA run used a single MER image for training. Each training image was compressed by the 2/6 wavelet's forward transform, subjected to 64:1 quantization, and then dequantized. The goal of each training run was to evolve a reconstruction transform that is capable of minimizing the MSE in reconstructed MER images. Each run used the following control parameters:

(a) Population size M = 50.
(b) Number of generations G = 500.
(c) Crossover percentage p_c = 85%.
(d) Mutation is Gaussian with Standard deviation = 0.3 and Shrink rate = 1.
(e) Elitism = 2 (i.e., the two best individuals from each generation are copied, unchanged, into the next generation, thus guaranteeing no decrease in the best individual's fitness from one generation to the next).

Each candidate solution consisted of 8 floating-point values. The initial population for each run (generation 0) was seeded with one exact copy and M-1 randomly mutated copies of the scaling and wavelet numbers from the 2/6 wavelet's reconstruction transform. At the conclusion of each training run, the best-of-run optimized reconstruction transform was applied to compressed, quantized, and dequantized versions of each of the remaining images from the test set.

The results for the five best floating-point transforms are tabulated in Fig. 2, while Fig. 3 shows results for the five best integer transforms. These results clearly support the following conclusions:

(a) Our GA is capable of optimizing the wavelet and scaling numbers describing transforms that consistently outperform the 2/6 wavelet for the reconstruction of deep space images under conditions subject to quantization error.

(b) Subject to the limited size of the training runs performed for this research, the GA consistently achieved greater improvement for the integer 2/6 transforms used by MER spacecraft than for more complex floating-point 2/6 transforms.

Training Image	Mean Improvement (test set)
MER7	6.60% (0.297 dB)
MER34	6.59% (0.296 dB)
MER42	6.58% (0.296 dB)
MER2	6.54% (0.294 dB)
MER36	6.49% (0.291 dB)

Figure 2. Average MSE Reduction, Evolved Floating-Point Transforms

Training Image	Mean Improvement (test set)
MER24	9.35% (0.426 dB)
MER39	9.16% (0.417 dB)
MER47	9.00% (0.410 dB)
MER36	8.98% (0.409 dB)
MER17	8.94% (0.407 dB)

Figure 3. Average MSE Reduction, Evolved Integer Transforms

Fig. 4 shows the five best training images for floating-point transforms, while Fig. 5 shows the five best for integer transforms. Note that the best images for training floating-point transforms are typically NOT the same as the best images for training integer transforms: in fact, only one training image (MER36) ranked in the top five for both types of transforms.

Fig. 6 shows the wavelet and scaling numbers comprising the best-of-run floating-point transform for each of the five training runs summarized by Fig. 2 (rounded to 4 decimal places), as well as the percentage change in the magnitude of each number relative to the corresponding value from the 2/6 wavelet. First, note that *none* of the evolved floating-point wavelet and scaling numbers changed sign relative to the original 2/6 wavelet. Second, note that the magnitude of 37 out of 40 of these evolved numbers (92.5%) decreased. Consistently, the largest magnitude changes occurred in the second wavelet number of the high-pass synthesis filter *g2*, as well as the first four scaling numbers of the low-pass synthesis filter *h2*; the last two scaling numbers of *h2* remained virtually unchanged for all runs, while the first wavelet number of *g2* either changed little, or changed considerably less than the second wavelet number. This result gives insight into how the GA is learning to compensate for the detrimental effects of quantization.

Fig. 7 shows the best-of-run wavelet and scaling numbers evolved from the integer 2/6 wavelet, and again shows the percentage change in the magnitude of each number relative to the corresponding value from that wavelet. Since images are reconstructed *after* transmission from MERs, it is unnecessary to reduce computational complexity on the receiving end (e.g., to reduce power consumption). Thus, we are free to evolve floating-point reconstruction filters to match the integer 2/6 compressor. As we observed previously, 36 of the 40 wavelet and scaling numbers for these five evolved transforms have decreased in magnitude. Large changes in the first four scaling numbers of *h2*, and negligible changes to the last two scaling numbers of *h2*, also mirror our results for floating-point transforms. On the other hand, changes to *g2* were inconsistent: in runs 2 and 4, greater changes occurred for the second wavelet number (as was observed for floating-point transforms), but in runs 1, 3, and 5, the largest magnitude changes occurred to the first wavelet number. In addition, *all eight* of the wavelet and scaling numbers have changed sign, in *all five* training runs. While it is well known that the behavior of commonly used wavelets (such as the 9/7 transform) is unaffected by the negation of all of the wavelet and scaling numbers defining the transforms, it is nevertheless quite surprising to find that all five of the runs evolving integer transforms negated all eight numbers, in light of the fact that none of the runs evolving floating-point transforms did so, and especially in light of the fact that the negation of any subset of these numbers will almost uniformly have a negative effect upon overall transform fitness.

Fig. 8 shows the image MER24 [Fig. 5(a)] after reconstruction by the integer 2/6 wavelet, while Fig. 9 shows the same image after reconstruction by the best transform evolved from the integer 2/6. These images remind us that MSE reductions over even 9% are difficult to discern with the naked eye. To better visualize MSE reduction, we created difference images by first eliminating the smallest 40% of the intensity values from each reconstructed image, and then multiplying the result by 10. Fig. 10 is the difference image derived from Fig. 8, while Fig. 11 was similarly derived from Fig. 9. The vastly smaller numbers and reduced intensity of white dots in Fig. 11 emphasize the extent to which the evolved transform has reduced MSE in comparison to the integer 2/6 wavelet.

IV. Comparative Results: D4 and 9/7

The results of the previous section demonstrated that it is possible to seed the initial population with randomly mutated copies of the 2/6 wavelet and evolve transforms that outperform the 2/6 for reconstruction of MER images previously compressed by the 2/6 under conditions subject to quantization error. This result raised the following question: is it possible to seed the population using a different wavelet and evolve a transform with even better performance on this class of images?

To answer this question, two additional sets of experiments were performed; the first set seeded the population with randomly mutated copies of the Daubechies-4 (D4) wavelet inverse transform, whose wavelet and scaling numbers (rounded to 4 digits) are:

h2 = {0.4830, 0.8365, 0.2241, -0.1294}

g2 = {-0.1294, -0.2241, 0.8365, -0.4830}

As with the 2/6 wavelet, 50 independent training runs were performed, with each run using a different training image. The

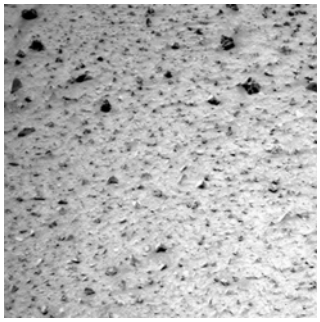

(a) MER7 (best training image)

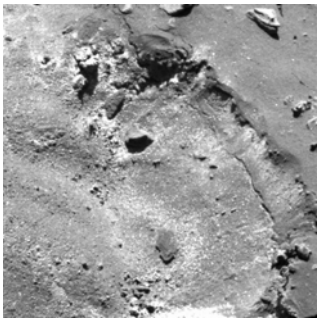

(b) MER34 (second best)

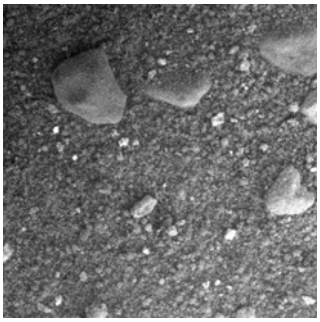

(c) MER42 (third best)

(d) MER2 (fourth best)

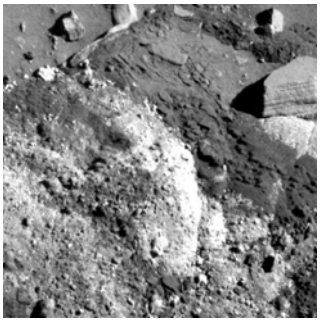

(e) MER36 (fifth best)

Figure 4. The five best training images for Floating-Point Transforms.

(a) MER24 (best training image)

(b) MER39 (second best)

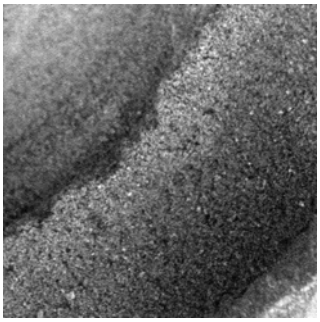

(c) MER47 (third best)

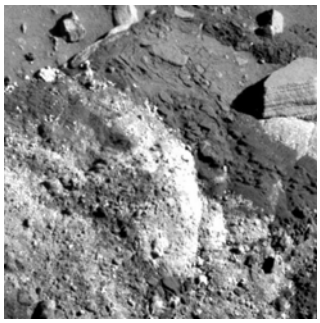

(d) MER36 (fourth best)

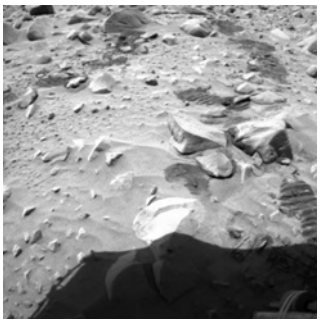

(e) MER17 (fifth best)

Figure 5. The five best training images for Integer Transforms.

Run	Evolved Numbers (% change in magnitude)
1	*h2* = [0.5045 (-28.7%), -0.5278 (-25.4%), 0.0338 (-61.8%), 0.0675 (-23.6%), 0.7061 (-0.14%), 0.7061 (-0.14%)]
	g2 = [-0.0870 (-1.57%), -0.0212 (-76.01%)]
2	*h2* = [0.5013 (-29.1%), -0.5127 (-27.5%), 0.0378 (-57.2%), 0.1051 (18.9%), 0.7062 (-0.13%), 0.7058 (-0.18%)]
	g2 = [-0.0895 (1.26%), -0.0572 (-35.3%)]
3	*h2* = [0.5067 (-28.3%), -0.4885 (-30.9%), 0.0494 (-44.1%), 0.0715 (-19.1%), 0.7050 (-0.30%), 0.7045 (-0.37%)]
	g2 = [-0.0632 (-28.4971%), -0.0341 (-61.4201%)]
4	*h2* = [0.5262 (-25.6%), -0.5118 (-27.6%), 0.0890 (0.69%), 0.0489 (-44.7%), 0.7058 (-0.18%), 0.7057 (-0.20%)]
	g2 = [-0.0829 (-6.21%), -0.0468 (-47.05%)]
5	*h2* = [0.4719 (-33.3%), -0.5008 (-29.2%), 0.0571 (-35.4%), 0.0840 (-4.96%), 0.7069 (-0.03%), 0.7047 (-0.34%)]
	g2 = [-0.0736 (-16.73%), -0.0619 (-29.97%)]

Figure 6. Wavelet and Scaling Numbers Evolved from Floating-point Transforms (% Magnitude Change from 2/6).

Run	Evolved Numbers (% change in magnitude)
1	*h2* = [-0.6852 (-31.5%), 0.6812 (-31.9%), -0.0639 (-48.9%), -0.1285 (2.80%), -0.4991 (-0.18%), -0.4994 (-0.12%)]
	g2 = [0.1031 (-17.52%), 0.1214 (-2.88%)]
2	*h2* = [-0.7071 (-29.3%), 0.6959 (-30.4%), -0.1110 (-11.2%), -0.0752 (-39.8%), -0.4999 (-0.02%), -0.4998 (-0.04%)]
	g2 = [0.1249 (-0.08%), 0.1119 (-10.48%)]
3	*h2* = [-0.7288 (-27.1%), 0.7304 (-27.0%), -0.1068 (-14.6%), -0.1059 (-15.3%), -0.4986 (-0.28%), -0.4997 (-0.06%)]
	g2 = [0.0650 (-48.00%), 0.0984 (-21.28%)]
4	*h2* = [-0.6374 (-36.3%), 0.6493 (-35.1%), -0.0391 (-68.7%), -0.1526 (22.1%), -0.5004 (0.08%), -0.4984 (-0.32%)]
	g2 = [0.1114 (-10.88%), 0.0745 (-40.40%)]
5	*h2* = [-0.6852 (-31.5%), 0.7394 (-26.1%), -0.0845 (-32.4%), -0.1597 (27.8%), -0.4991 (-0.18%), -0.4999 (-0.02%)]
	g2 = [0.0550 (-56.00%), 0.1123 (-10.16%)]

Figure 7. Wavelet and Scaling Numbers Evolved from Integer Transforms (% Magnitude Change from 2/6).

Figure 8. A typical MER image (MER24) reconstructed by the integer 2/6 transform.

Figure 9. The same image reconstructed by the best evolved transform. MSE reductions as large as 9% are very difficult to see with the naked eye.

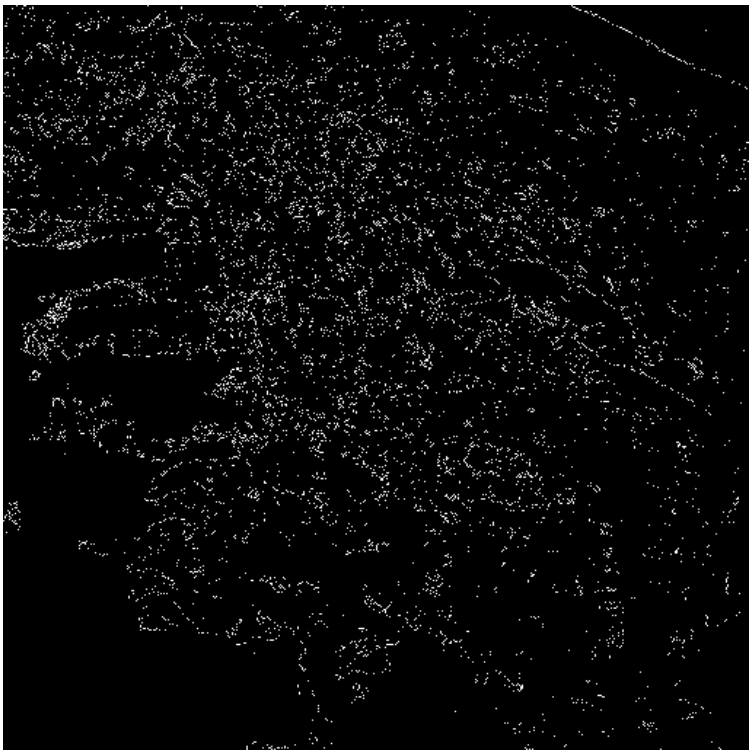

Figure 10. The difference image for the integer 2/6. Error is proportional to the number and intensity of lighter dots.

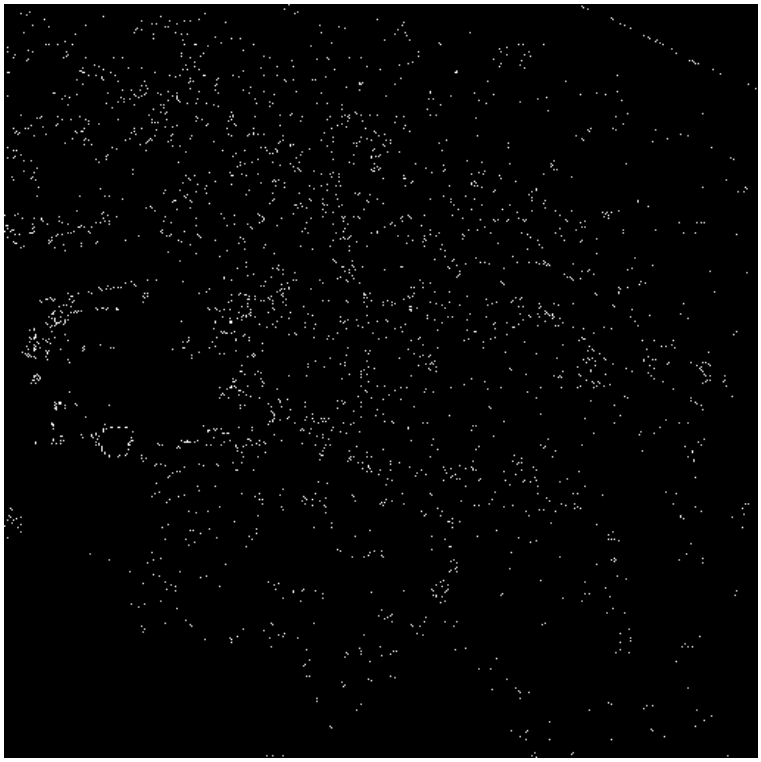

Figure 11. The difference image for the best transform evolved from the integer 2/6. The much smaller number and reduced intensity of dots is indicative of substantially reduced MSE.

best-of-run transforms were subsequently tested against the remaining 49 images from the test set. In comparison to the three best transforms evolved using the integer 2/6 wavelet to seed the initial population, the best transform evolved from the D4 introduced an average of *at least 25% greater MSE*. This result clearly indicates that the integer 2/6 is by far a better choice than the D4 for seeding the initial population in order to evolve a superior MER image reconstruction transform.

The second set of experiments seeded the initial population using 9/7 inverse transform, whose wavelet and scaling numbers (rounded to 4 digits) are:

h2 = [-0.0645, -0.0407, 0.4181, 0.7885, 0.4181, -0.0407, -0.0645]

g2 = [0.0378, 0.0239, -0.1106, -0.3774, 0.8527,-0.3774, -0.1106, 0.0239, 0.0378]

50 best-of-run transforms were tested against 50 MER images. The best transform evolved from the 9/7 introduced *at least 20% greater average MSE* into MER images than the three best transforms evolved from the integer 2/6. This result would again seem to indicate the superiority of the integer 2/6 as a starting point for evolving a MER image reconstruction transform; however, an additional factor should be considered: although the scale of each training run (M = 50, G = 500) appears to have been sufficient to allow transforms evolved from either the integer 2/6 or D4 wavelet to converge towards an optimized solution, it is plausible that larger runs may be necessary to evolve transforms from the much more complex 9/7. The much greater variation in the wavelet and scaling numbers of transforms evolved from the 9/7 may be the result of the problem's higher dimensionality.

V. Conclusions and Future Research

The research described in this paper clearly establishes that GAs are capable of evolving transforms that outperform the most commonly used ICER wavelet for the reconstruction of MER images under conditions subject to quantization error. At 64:1 quantization, the best evolved floating-point transform reduced MSE by an average of 6.60% (0.297 dB) and 9.35% (0.426 dB), respectively, in comparison to floating-point and integer versions of the 2/6 wavelet.

As a next step, the wavelet and scaling numbers of the 2/6 wavelet used by the software implementation of ICER [8] should be replaced with those of the best-of-run evolved transform. The resulting system should then be applied to actual ICER images in order to further validate the results of this study.

It is likely that the relatively small scale of the runs performed for this study (M = 50, G = 500), and the use of a single training image per run, limited the performance enhancement of best-of-run transforms in comparison to the2/6 wavelets. Future research will include much larger populations, longer training runs, and various combinations of two or more training images in order to achieve greater improvements. In addition, evolving larger populations for a much greater number of generations may allow transforms evolved from the 9/7 wavelet to achieve reconstruction performance comparable to transforms evolved from the 2/6.

As mentioned above, an advantage to the approach described in this paper is that it requires only the reconstruction filter to be modified, i.e., no changes to deployed image compressors are necessary. Thus, this approach is especially useful for deployed systems in which the compressor has been implemented in hardware. Nevertheless, our prior experience with photographs [2], fingerprints [3], and satellite images [4] demonstrated that additional MSE reduction may be achieved by simultaneously evolving wavelet and scaling numbers for both the forward and inverse transform. Future research should apply this approach to deep space images. Evolving both compression and reconstruction transforms will be particularly beneficial for missions (such as the MERs) that use a software implementation of ICER for all lossy image compression [8]. In addition, the modified GA should allow the user to evolve either integer or floating-point compression transforms.

For this research, lossy compression was achieved using 64:1 uniform scalar quantization. Future research should specifically address the "subband quantization with a dead zone" scheme [7] employed on MER missions, and other more commonly used quantization algorithms [6]. In addition, the transforms evolved during this research performed a single stage of decomposition; however, most wavelet-based image compression systems (including ICER) use the MRA scheme [9] to achieve much greater compression. Future research should extend the current GA to evolve MRA transforms having different sets of wavelet and scaling numbers for each compression and reconstruction transform at each stage of decomposition [11].

As mentioned above, the ICER image compressor is used for other NASA missions, including STEREO [12] and EO-1 [13]. Future research should investigate whether our approach could be extended to support these missions. In particular, we should attempt to identify techniques for improved compression and reconstruction of multispectral and hyperspectral images.

Acknowledgment

This research was partially funded through the Alaska Space Grant Program. Some of the training runs for this research were completed using high-performance computing resources made available by the Arctic Region Supercomputer Center (ARSC) in Fairbanks, AK; the authors are grateful for the assistance from numerous ARSC staff members throughout this project. Fig. 1 (PIA 04413) was obtained from the online JPL photojournal and is credited to NASA/JPL and Cornell University.

References

[1] M. Adams and F. Kossentini, "Reversible integer-to-integer wavelet transforms for image compression: performance evaluation and analysis," IEEE Trans. Image Proc., vol. 9(7), pp. 1010-1024, 2000.

[2] B. Babb, S. Becke, and F. Moore, “Evolving Optimized Matched Forward and Inverse Transform Pairs via Genetic Algorithms,” Proc. 48th IEEE Int. Midwest Symp. Circuits and Systems: Cincinnati, OH, 8/7-10, 2005.
[3] B. Babb, F. Moore, M. Peterson, and G. Lamont, “Improved Satellite Image Compression and Reconstruction via Genetic Algorithms,” Electro-Optical Remote Sensing, Photonic Technologies, and Applications II, SPIE Symp. Optics/Photonics in Security & Defence, Cardiff, UK, 9/15-18, 2008.
[4] B. Babb, F. Moore, and M. Peterson, “Improved Multiresolution Analysis Transforms for Satellite Image Compression and Reconstruction using Evolution Strategies,” Proc. Eleventh Annual Genetic and Evolutionary Computation Conf., Montreal, QC, Canada, 7/8-12, 2009.
[5] Cohen, A., I. Daubechies, and J. Feauveau, “Biorthogonal Bases of Compactly Supported Wavelets,” Comm. Pure and Applied Mathematics, vol. 45, pp. 485-560, 1992.
[6] P. Cosman, R. Gray, and M. Vetterli, “Vector Quantization of Image Subbands: A Survey,” IEEE Trans. Image Proc., vol. 5(2), pp. 202-225, 1996.
[7] H. Gharavi and A. Tabatabai, “Subband Coding of Monochrome and Color Image,” IEEE Trans. Circuits and Systems, vol. 35(2), pp. 207-214, 1988.
[8] A. Kiely and M. Klimesh, “The ICER Progressive Wavelet Image Compressor,” IPN Progress Report 42-155, November 15, 2003.
[9] S. Mallat, A Wavelet Tour of Signal Processing (2nd Ed.), Academic Press, 1999.
[10] F. Moore, P. Marshall, and E. Balster, “Evolved Transforms for Image Reconstruction,” Proc. IEEE Congress on Evolutionary Computation, Edinburgh, Scotland, UK, 9/02-05, 2005.
[11] F. Moore, “A Genetic Algorithm for Evolving Improved MRA Transforms,” WSEAS Trans. Signal Proc., vol. 1 (1), pp. 97-104, 2005.
[12] C. Russell (Ed.), The STEREO Mission, Springer, 2008.
[13] S. Ungar, J. Pearlman, J. Mendenhall, and D. Reuter, “Overview of the Earth Observing One (EO-1) Mission,” IEEE Trans. Geosciences and Remote Sensing, vol. 41, pp. 1149-1159, 2003.
[14] A. Zandi, D. Allen, E. Schwartz, and M. Boliek, “CREW: Compression with Reversible Embedded Wavelets,” Proc. IEEE Data Compression Conf., pp. 212-221, 1995.